

University of Wollongong

Research Online

Faculty of Engineering and Information
Sciences - Papers: Part A

Faculty of Engineering and Information
Sciences

1-1-2017

Osmotic versus conventional membrane bioreactors integrated with reverse osmosis for water reuse: biological stability, membrane fouling, and contaminant removal

Wenhai Luo

University of Wollongong, wl344@uowmail.edu.au

Hop Phan

University of Wollongong, vhp997@uowmail.edu.au

Ming Xie

University of Melbourne, mx504@uowmail.edu.au

Faisal I. Hai

University of Wollongong, faisal@uow.edu.au

William E. Price

University of Wollongong, wprice@uow.edu.au

See next page for additional authors

Follow this and additional works at: <https://ro.uow.edu.au/eispapers>



Part of the [Engineering Commons](#), and the [Science and Technology Studies Commons](#)

Research Online is the open access institutional repository for the University of Wollongong. For further information contact the UOW Library: research-pubs@uow.edu.au

Osmotic versus conventional membrane bioreactors integrated with reverse osmosis for water reuse: biological stability, membrane fouling, and contaminant removal

Abstract

This study systematically compares the performance of osmotic membrane bioreactor - reverse osmosis (OMBR-RO) and conventional membrane bioreactor - reverse osmosis (MBR-RO) for advanced wastewater treatment and water reuse. Both systems achieved effective removal of bulk organic matter and nutrients, and almost complete removal of all 31 trace organic contaminants investigated. They both could produce high quality water suitable for recycling applications. During OMBR-RO operation, salinity build-up in the bioreactor reduced the water flux and negatively impacted the system biological treatment by altering biomass characteristics and microbial community structure. In addition, the elevated salinity also increased soluble microbial products and extracellular polymeric substances in the mixed liquor, which induced fouling of the forward osmosis (FO) membrane. Nevertheless, microbial analysis indicated that salinity stress resulted in the development of halotolerant bacteria, consequently sustaining biodegradation in the OMBR system. By contrast, biological performance was relatively stable throughout conventional MBR-RO operation. Compared to conventional MBR-RO, the FO process effectively prevented foulants from permeating into the draw solution, thereby significantly reducing fouling of the downstream RO membrane in OMBR-RO operation. Accumulation of organic matter, including humic- and protein-like substances, as well as inorganic salts in the MBR effluent resulted in severe RO membrane fouling in conventional MBR-RO operation.

Keywords

osmosis, reverse, integrated, bioreactors, membrane, conventional, versus, contaminant, fouling, stability, osmotic, biological, removal, reuse:, water

Disciplines

Engineering | Science and Technology Studies

Publication Details

Luo, W., Phan, H. V., Xie, M., Hai, F. I., Price, W. E., Elimelech, M. & Nghiem, L. D. (2017). Osmotic versus conventional membrane bioreactors integrated with reverse osmosis for water reuse: biological stability, membrane fouling, and contaminant removal. *Water Research*, 109 122-134.

Authors

Wenhai Luo, Hop Phan, Ming Xie, Faisal I. Hai, William E. Price, Menachem Elimelech, and Long D. Nghiem

1 **Osmotic versus conventional membrane bioreactors integrated**
2 **with reverse osmosis for water reuse: Biological stability,**
3 **membrane fouling, and contaminant removal**

4 Fresh manuscript submitted to *Water Research*

5 November 2016

6 Wenhai Luo ^a, Hop V. Phan ^a, Ming Xie ^b, Faisal I. Hai ^a, William E. Price ^c, Menachem
7 Elimelech ^d, Long D. Nghiem ^{a*}

8 ^a Strategic Water Infrastructure Laboratory, School of Civil, Mining and Environmental
9 Engineering, University of Wollongong, Wollongong, NSW 2522, Australia

10 ^b Institute for Sustainability and Innovation, College of Engineering and Science, Victoria
11 University, Melbourne, VIC 8001, Australia

12 ^c Strategic Water Infrastructure Laboratory, School of Chemistry, University of Wollongong,
13 Wollongong, NSW 2522, Australia

^d Department of Chemical and Environmental Engineering, Yale University, New Haven,
Connecticut 06520-8286, United States

* Corresponding author: longn@uow.edu.au; Ph: +61 (2) 4221 4590.

14 **Abstract**

15 This study systematically compares the performance of osmotic membrane bioreactor –
16 reverse osmosis (OMBR-RO) and conventional membrane bioreactor – reverse osmosis
17 (MBR-RO) for advanced wastewater treatment and water reuse. Both systems achieved
18 effective removal of bulk organic matter and nutrients, and almost complete removal of all 31
19 trace organic contaminants investigated. They both could produce high quality water suitable
20 for recycling applications. During OMBR-RO operation, salinity build-up in the bioreactor
21 reduced the water flux and negatively impacted the system biological treatment by altering
22 biomass characteristics and microbial community structure. In addition, the elevated salinity
23 also increased soluble microbial products and extracellular polymeric substances in the mixed
24 liquor, which induced fouling of the forward osmosis (FO) membrane. Nevertheless,
25 microbial analysis indicated that salinity stress resulted in the development of halotolerant
26 bacteria, maintaining the OMBR system biologically active. By contrast, biological
27 performance was relatively stable throughout conventional MBR-RO operation. Compared to
28 conventional MBR-RO, the FO process effectively prevented foulants from permeating into
29 the draw solution, thereby significantly reducing fouling of the downstream RO membrane in
30 OMBR-RO operation. Accumulation of organic matter, including humic- and protein-like
31 substances, as well as inorganic salts in the MBR effluent resulted in severe RO membrane
32 fouling in conventional MBR-RO operation.

33 **Keywords:** Osmotic membrane bioreactor (OMBR); forward osmosis (FO); reverse osmosis
34 (RO); trace organic contaminants (TrOCs); membrane fouling.

35 **1. Introduction**

36 Water scarcity due to population growth, urbanization, climate change, and environmental
37 pollution is a vexing challenge to the sustainable development of our society (Elimelech and
38 Phillip, 2011). This challenge calls for further efforts to develop and improve technologies
39 that can tap into alternative water sources, such as municipal wastewater, to enhance water
40 supply and mitigate water shortage. The ubiquitous presence of trace organic contaminants
41 (TrOCs) in reclaimed water and wastewater-impacted water bodies remains a major obstacle
42 to water reuse. TrOCs are emerging organic chemicals of significant concerns derived from
43 either anthropogenic or natural activities as they present potential health risks to humans and
44 other living organisms (Luo et al., 2014b).

45 Membrane bioreactor (MBR) is a well-known technology for wastewater treatment and water
46 reuse. MBR combines conventional activated sludge (CAS) treatment and a physical
47 membrane filtration process, typically including microfiltration (MF) and ultrafiltration (UF).
48 As an alternative to CAS treatment, MBR is more robust and versatile and can produce
49 higher standard effluent with smaller sludge production and physical footprint (Hai et al.,
50 2014). Some evidence has emerged that MBR could enhance the removal of TrOCs,
51 particularly moderately biodegradable and hydrophobic compounds compared to CAS
52 treatment (Clara et al., 2005; De Wever et al., 2007). However, some hydrophilic TrOCs are
53 still poorly removed by MBR due to their resistance to biodegradation and low adsorption
54 onto sludge (Tadkaew et al., 2011; Nguyen et al., 2013; Wijekoon et al., 2013). Thus, further
55 treatment by nanofiltration (NF) or reverse osmosis (RO) is usually required to produce high
56 quality water for reuse (Gerrity et al., 2013). The NF/RO process can complement well MBR
57 to achieve effective removal of various TrOCs (Alturki et al., 2010; Nguyen et al., 2013).

58 Recent progress in water reuse has led to the emergence of a new variation of MBR, namely,
59 osmotic membrane bioreactor (OMBR) (Achilli et al., 2009; Cornelissen et al., 2011; Chen et
60 al., 2014; Nguyen et al., 2016). During OMBR operation, treated water is extracted from the
61 mixed liquor into a highly concentrated draw solution by the forward osmosis (FO) process.
62 By employing a selective, semi-permeable FO membrane, TrOCs can be retained in the
63 bioreactor and thus increase their biodegradation during OMBR operation (Alturki et al.,
64 2012; Holloway et al., 2014). Moreover, FO has a lower fouling propensity, and when
65 fouling occurs, it is readily reversible compared to pressure-driven membrane processes (Mi
66 and Elimelech, 2010; Kim et al., 2014; Luo et al., 2015a; Xie et al., 2015).

67 OMBR can be used as a stand-alone process or coupled with a desalination process, such as
68 RO to form an OMBR-RO hybrid system, for draw solution recovery and recycling water
69 production (Luo et al., 2014a). In the latter configuration, the desalination process may
70 provide an additional barrier to further purify the product water. For instance, Holloway et al.
71 (2014) demonstrated that 15 of 20 TrOCs detected in municipal wastewater were removed to
72 below detection limit by OMBR, and compounds that passed through the FO membrane were
73 effectively retained by the subsequent RO process. An effective contaminant removal by
74 OMBR-RO and its potential for advanced wastewater treatment and water reuse were also
75 subsequently highlighted by Luo et al. (2016b). It is noteworthy that an MF or UF membrane
76 was coupled with OMBR in these two studies to control salinity build-up, which is an
77 inherent issue associated with OMBR due to the high salt rejection by the FO membrane and,
78 more importantly, the reverse draw solute flux.

79 OMBR-RO can offer a range of potential benefits over conventional MBR-RO systems for
80 advanced wastewater treatment and water reuse. Cornelissen et al. (2011) reported that
81 OMBR-RO could reduce the capital cost of wastewater reuse by 5 – 25% compared to
82 conventional MBR-RO using the UF membrane. Cost saving achieved by OMBR-RO

83 depends on the assumption that the cost and water permeability of the FO membrane are
84 comparable to those of the UF membrane. Given the low fouling property of FO compared to
85 UF, there can be also a reduction in operational cost related to membrane cleaning and
86 replacement. Cornelissen et al. (2011) also assumed that the two hybrid systems had the same
87 treatment performance, which was probably conservative as the FO membrane can produce
88 higher quality permeate than the UF membrane. The high quality FO permeate would
89 alleviate membrane fouling in the downstream RO process, which is a major issue for cost-
90 effective application of conventional OMBR-RO for water reuse (Farias et al., 2014; Al
91 Ashhab et al., 2014). Thus, additional cost saving for OMBR-RO can potentially be derived
92 from a more stable water production from the downstream RO unit with less frequent
93 cleaning and longer service time in comparison with conventional MBR-RO. Of a particular
94 note, to date, no study has directly compared the performance of OMBR-RO and
95 conventional MBR-RO for water reuse.

96 This study aims to compare the performance of OMBR-RO with conventional MBR-RO in
97 terms of biological stability, contaminant removal, and membrane fouling. Similar operating
98 parameters were applied to both bioreactors for a systematic comparison. Water production
99 and salinity build-up during OMBR-RO operation were evaluated. High-throughput
100 sequencing technique was applied to elucidate the effect of salinity build-up on microbial
101 community structure during OMBR-RO operation compared to that in conventional MBR-
102 RO. Fate and transport behaviours of bulk organic matter, nutrients, and TrOCs in these two
103 hybrid systems were systematically examined. In addition, the fouling behaviour of the RO
104 membrane in both systems was also delineated and compared.

105 **2. Materials and methods**

106 *2.1 Synthetic wastewater and trace organic contaminants*

107 A synthetic wastewater was used in this study. The synthetic wastewater was prepared daily
108 to obtain 100 mg/L glucose, 100 mg/L peptone, 17.5 mg/L KH_2PO_4 , 17.5 mg/L MgSO_4 , 10
109 mg/L FeSO_4 , 225 mg/L CH_3COONa , and 35 mg/L urea (Alturki et al., 2010).

110 A set of 31 TrOCs were selected to represent four major groups of emerging organic
111 chemicals of significant concern — endocrine disrupting compounds, pharmaceutical and
112 personal care products, industrial chemicals, and pesticides — that occur ubiquitously in
113 municipal wastewater. Key physicochemical properties of these TrOCs are summarized in
114 Table S1, Supplementary Data. Based on their effective octanol – water partition coefficient
115 (i.e. Log D) at solution pH 8, the 31 TrOCs could be categorized as hydrophobic (i.e. Log D
116 > 3.2) and hydrophilic (i.e. Log D < 3.2) (Tadkaew et al., 2011). A stock solution containing
117 25 $\mu\text{g/mL}$ of each of TrOCs was prepared in pure methanol and stored at $-18\text{ }^\circ\text{C}$ in the dark.
118 The stock solution was introduced into the synthetic wastewater described above to obtain a
119 concentration of 5 $\mu\text{g/L}$ of each compound. The TrOC stock solution was used within a
120 month.

121 *2.2 Experimental systems*

122 *2.2.1 Osmotic membrane bioreactor – reverse osmosis*

123 A lab-scale OMBR-RO system was used (Figure S1a, Supplementary Data). This hybrid
124 system was consisted of a feed solution reservoir, a glass bioreactor with a submerged, plate-
125 and-frame FO membrane cell, a draw solution reservoir, and a cross-flow RO unit. A water
126 level controller was used to regulate a Masterflex peristaltic pump (Cole-Parmer, Vernon
127 Hills, IL) to feed the bioreactor. The feed reservoir was positioned on a digital balance

128 (Mettler-Toledo, Hightstown, IL), which was connected to a computer. A decrease in the feed
129 reservoir weight was recorded and then used to calculate the FO water flux.

130 The FO membrane cell was made of acrylic plastic. A flat-sheet, thin-film composite (TFC)
131 FO membrane was mounted on the cell to seal the draw solution flow channel of 20 cm long,
132 15 cm wide, and 0.4 cm high. The membrane active layer was in contact with the mixed
133 liquor (i.e. FO mode) with an effective surface area of 300 cm². The draw solution was
134 circulated from a stainless steel reservoir to the membrane cell by a gear pump (Micropump,
135 Vancouver, WA) at a cross-flow velocity of 2.8 cm/s.

136 The TFC FO membrane used in this study was obtained from Hydration Technology
137 Innovations (Albany, OR). Similar to TFC FO membranes from other suppliers (e.g. Oasys
138 Water and Porifera), this membrane comprised a thin, selective polyamide active layer and a
139 porous polysulfone support layer. These TFC FO membranes have higher rejection capacity
140 and much higher water permeability than cellulose triacetate based FO membranes (Cath et
141 al., 2013). In fact, TFC FO membranes with two to three times higher water permeability
142 than the membrane used in this study have been recently reported (Tian et al., 2015; Wei et
143 al., 2015). It is noted that the polyamide active layer of commercial membranes can be
144 slightly modified by proprietary additives. In addition, the support layer structure can also
145 influence the membrane water permeability (Lu et al., 2015). However, this study was
146 specific to the comparison between OMBR and conventional MBR, rather than membrane
147 properties. Thus, findings from this study are still valid to OMBR using other FO
148 membranes.

149 The cross-flow RO unit, comprising a Hydra-Cell high pressure pump (Wanner Engineering,
150 Minneapolis, MN) and a membrane cell made of stainless steel, was coupled with OMBR to
151 reconcentrate the draw solution and produce recycling water. A flat-sheet, TFC polyamide
152 RO membrane (LFC3, Hydranautics, Oceanside, CA) was embedded into the membrane cell

153 with a flow channel height of 0.2 cm and an effective membrane surface area of 40 cm² (4 cm
154 × 10 cm). A bypass valve and a back-pressure regulator (Swagelok, Solon, OH) were used to
155 adjust the hydraulic pressure and cross-flow velocity. A temperature controller (Neslab
156 RTE7, Waltham, MA) installed with a stainless steel heat exchanger coil was used to
157 maintain the RO feed (i.e. OMBR draw solution) temperature at 21 ± 1 °C. Water flux was
158 monitored by a digital flow meter (Optiflow, Palo Alto, CA), which was connected to a
159 computer. Key properties of the FO and RO membranes used in the OMBR-RO hybrid
160 system are provided in Table S2, Supplementary Data.

161 2.2.2 *Conventional membrane bioreactor – reverse osmosis*

162 A lab-scale, conventional MBR-RO system was composed of a hollow fibre MF membrane
163 module (Mitsubishi Rayon Engineering, Tokyo, Japan) in a glass bioreactor and an RO unit
164 (Figure S1b, Supplementary Data). The bioreactor and RO unit were identical to those used
165 in the OMBR-RO system. The MF membrane was made of polyvinylidene fluoride with a
166 nominal pore size and an effective surface area of 0.4 µm and 740 cm², respectively. The MF
167 membrane driven by a Masterflex peristaltic pump (Cole-Parmer, Vernon Hills, IL) was
168 operated in a cycle of 14 min suction and 1 min relaxation. The relaxation time was set to
169 reduce membrane fouling. A high resolution (±0.1 kPa) pressure sensor (Extech Equipment,
170 Australia) was installed to record the trans-membrane pressure (TMP).

171 2.3 *Experimental protocol*

172 Activated sludge from the Wollongong Wastewater Treatment Plant (Wollongong, Australia)
173 was used to inoculate the two bioreactors. The bioreactors were acclimatized to the synthetic
174 wastewater described above for over 60 days using MF membranes for effluent extraction
175 under the same conditions. Once acclimatized with regards to bulk organic removal (i.e. over
176 97% total organic carbon (TOC) removal), the MF membrane was removed from one

177 bioreactor, which was then integrated with the FO and RO components to form the OMBR-
178 RO hybrid system. A same RO component was coupled with the other bioreactor to establish
179 the conventional MBR-RO system.

180 Both OMBR-RO and conventional MBR-RO systems were continuously operated for 40
181 days under similar conditions in a constant temperature room (22 ± 1 °C). The bioreactors
182 with working volume of 6 L were continuously aerated to obtain a mixed liquor dissolved
183 oxygen (DO) concentration of 5 ± 1 mg/L. The initial mixed liquor suspended solids (MLSS)
184 concentration was adjusted to approximately 5 g/L. The sludge retention time (SRT) was
185 controlled at 20 days by daily wasting 300 mL mixed liquor. The hydraulic retention time
186 (HRT) was in the range of 27 – 60 hours determined by the water flux of OMBR. A 0.5 M
187 NaCl draw solution (with effective volume of 10 L) was used for OMBR. On day 20, 100 g
188 NaCl was added to replenish draw solute loss caused by the reverse salt flux and its passage
189 through the downstream RO membrane. This amount was calculated based on a decrease in
190 the electrical conductivity of the draw solution and a NaCl calibration curve.

191 Water flux of the conventional MBR was adjusted daily to be equal to that of OMBR to
192 systematically compare their effects on the downstream RO process. At the same time, the
193 RO water flux was also adjusted accordingly by regulating the applied hydraulic pressure
194 while fixing the cross-flow velocity at 41.7 cm/s. As a result, the working volume of the draw
195 solution and MBR effluent was constant at 10 L over the entire experimental period. No
196 membrane cleaning was conducted for both systems during their operation. A new RO
197 membrane was used once its normalized water permeability decreased to 0.2.

198 2.4 Analytical methods

199 2.4.1 Measurement of basic water quality parameters

200 Basic water quality parameters were analysed every three days. Specifically, TOC and total
201 nitrogen (TN) were analysed using a TOC/TN analyser (TOC-V_{CSH}, Shimadzu, Kyoto).
202 Ammonium (NH₄⁺) and orthophosphate (PO₄³⁻) were determined by a Flow Injection
203 Analysis system (QuikChem 8500, Lachat, CO). An Orion 4-Star Plus pH/conductivity meter
204 (Thermo Scientific, Waltham, MA) was used to monitor the solution pH and electrical
205 conductivity on a daily basis.

206 2.4.2 Measurement of trace organic contaminants

207 Aqueous samples were taken from the OMBR-RO and MBR-RO systems every ten days for
208 TrOC analysis using a method previously described by Hai et al. (2011). Briefly, the method
209 involved solid phase extraction, derivatisation, and quantification by a gas chromatography –
210 mass spectrometry system (QP5000 GC-MS, Shimadzu, Kyoto).

211 In OMBR-RO, TrOC removal rates by the bioreactor (R_{Bio}), OMBR (R_{OMBR}), and OMBR-RO
212 ($R_{Overall}$) are defined as follows:

213
$$R_{Bio} = \left(1 - \frac{C_{Sup} V_{Bio} + C_{Draw}^* \Delta V_{FO}}{C_{Feed} \Delta V}\right) \times 100\% \quad (1)$$

214
$$R_{OMBR} = \left(1 - \frac{C_{Draw}^*}{C_{Feed}}\right) \times 100\% \quad (2)$$

215
$$R_{Overall} = \left(1 - \frac{C_{Permeate}}{C_{Feed}}\right) \times 100\% \quad (3)$$

216 where C_{Feed} , C_{Sup} , and $C_{Permeate}$ is the measured TrOC concentration (ng/L) in the feed, mixed
217 liquor supernatant, and RO permeate, respectively; C_{Draw}^* is the TrOC concentration in the
218 FO permeate; V_{Bio} is the effective bioreactor volume (i.e. 6 L); and ΔV_{FO} is the volume of

219 water passed through the FO membrane between time t and $t+\Delta t$. TrOCs accumulate in the
 220 draw solution when they pass through the FO membrane but are retained by the subsequent
 221 RO membrane (D'Haese et al., 2013). Thus, C_{Draw}^* is determined from a mass balance:

$$222 \quad C_{Draw}^* = \frac{M_{FO}}{Q_{FO}} \quad (4)$$

$$223 \quad M_{FO} = \frac{V_{Draw}(C_{Draw(t+\Delta t)} - C_{Draw(t)})}{\Delta t} + \frac{(C_{RO(t+\Delta t)} + C_{RO(t)})}{2} \Delta V \quad (5)$$

$$224 \quad \Delta V = Q_{RO} \Delta t \quad (6)$$

225 where M_{FO} is the mass flow rate of TrOCs crossed through the FO membrane; $C_{Draw(t)}$ and
 226 $C_{Draw(t+\Delta t)}$ is the measured TrOC concentration in the draw solution at time t and $t+\Delta t$,
 227 respectively; $C_{RO(t)}$ and $C_{RO(t+\Delta t)}$ is the measured TrOC concentration in the RO permeate at
 228 time t and $t+\Delta t$, respectively; and Q_{FO} and Q_{RO} is the water flux of the FO and RO
 229 membranes, respectively. As noted in Section 2.3, the RO water flux (Q_{RO}) was adjusted to
 230 be equal to that of the FO membrane (Q_{FO}). Based on eqs. (4) – (6), C_{Draw}^* is calculated from

$$231 \quad C_{Draw}^* = \frac{V_{Draw}(C_{Draw(t+\Delta t)} - C_{Draw(t)})}{\Delta V_{FO}} + \frac{(C_{RO(t+\Delta t)} + C_{RO(t)})}{2} \quad (7)$$

232 According to eqs. (1) – (3), the observed TrOC rejection rate by the FO ($R_{Ob FO}$) and RO ($R_{Ob RO}$)
 233 membranes is calculated as:

$$234 \quad R_{Ob FO} = R_{OMBR} - R_{Bio} \quad (8)$$

$$235 \quad R_{Ob RO} = R_{Overall} - R_{OMBR} \quad (9)$$

236 The observed TrOC rejection rate does not reflect the real separation capacity of the FO and
 237 RO membranes, but can be used to infer their contributions to TrOC removal in OMBR-RO.
 238 Similar to OMBR-RO operation, the RO water flux was adjusted daily to match the MBR

239 effluent flow rate, maintaining the effluent reservoir with a working volume of 10 L during
240 conventional MBR-RO operation (Section 2.3). Therefore, the calculation process listed
241 above was also applicable to evaluate TrOC removal by different compartments of
242 conventional MBR-RO.

243 *2.4.3 Fluorescence excitation – emission matrix spectroscopy*

244 Fluorescence intensities of the OMBR and MBR mixed liquor supernatant, draw solution,
245 and MBR effluent samples at the beginning and conclusion of OMBR-RO and conventional
246 MBR-RO operation were measured to determine organic substances likely responsible for
247 fouling of the RO membrane using a two-dimensional fluorescence spectrophotometer
248 (Perkin-Elmer LS-55) with excitation wavelengths between 240 and 450 nm and emission
249 wavelengths between 290 and 580 nm (in 5 nm increments). Samples were prepared and
250 analysed based on the method reported by Cory and McKnight (2005). Fluorophores detected
251 in certain areas of optical space in an excitation-emission-intensity matrix (EEM) correspond
252 to specific fractions of dissolved organic matter (Henderson et al., 2009; Xie and Gray, 2016).
253 All samples were diluted to a same TOC concentration for resolving and comparing EEM
254 spectra.

255 *2.4.4 Microbial community analysis*

256 Sludge samples were taken at the beginning and conclusion of OMBR and conventional
257 MBR operation for microbial community analysis according to a method reported previously
258 by Luo et al. (2016c). In brief, the method included DNA extraction using the FastDNA[®]
259 SPIN Kit for soil (MP Biomedicals, Santa Ana, CA), PCR amplification of V1 – V3 16S
260 rRNA gene, and amplicon sequencing on a Illumina MiSeq platform (Australian Genome
261 Research Facility, Queensland, Australia).

262 Paired-end reads were assembled using PEAR (version 0.9.8) (Zhang et al., 2014) and then
263 processed with Quantitative Insights into Microbial Ecology (QIIME 1.9.1) (Caporaso et al.,
264 2010), USEARCH (version 8.0.1623) (Edgar, 2013), and UPARSE pipeline. All sequencing
265 data here are available at the Sequence Read Archive (accession number: SRP072961) in the
266 National Centre for Biotechnology Information (Bethesda, MD).

267 2.4.5 *Biomass characterisation*

268 MLSS and mixed liquor volatile suspended solids (MLVSS) concentrations in the bioreactor
269 were analysed based on Standard Method 2540 (APHA, 2005). Biomass activity was
270 evaluated by determining the specific oxygen uptake rate (SOUR) of activated sludge using
271 Standard Method 1683 (APHA, 2005). Extracellular polymeric substance (EPS) in the sludge
272 were extracted using a method from Zhang et al. (1999). EPS and soluble microbial products
273 (SMP) in the mixed liquor were measured by analysing their protein and polysaccharide
274 concentrations. Proteins and polysaccharides were determined by the Folin method with
275 bovine serum albumin as the standard and the phenol-sulfuric acid method with glucose as
276 the standard, respectively (Semblante et al., 2015).

277 2.4.6 *Membrane autopsy*

278 At the conclusion of OMBR-RO and conventional MBR-RO operation, a scanning electron
279 microscopy (SEM) coupled with energy dispersive spectroscopy (EDS) (JCM-6000, JEOL,
280 Tokyo, Japan) was used to identify the morphology and composition of the fouling layer on
281 the membrane surface. Membrane samples were air-dried in a desiccator before being coated
282 with an ultra-thin gold layer with a sputter coater (SPI Module, West Chester, PA) for SEM
283 imaging. Attenuated Total Reflection – Fourier Transform Infrared (ATR-FTIR)
284 spectroscopy (IRAffinity-1, Shimadzu, Kyoto, Japan) was also used to probe the chemical
285 composition of the fouling layer. The measured spectrum ranged between 600 and 4000 cm^{-1}

286 with 2 cm⁻¹ resolution. Each scan was performed 20 times. A background correction was
287 conducted before each measurement.

288 **3. Results and discussion**

289 *3.1 Process performance*

290 *3.1.1 Mixed liquor salinity and water flux*

291 Salinity build-up in the bioreactor is an inherent issue associated with OMBR due to the
292 effective salt rejection by the FO membrane and the reverse draw solute flux. Thus, the
293 mixed liquor conductivity increased significantly within the first 10 days of OMBR operation
294 (Figure 1). Less significant conductivity increase was observed thereafter, which could be
295 attributed to a decrease in the reverse draw solute flux associated with the water flux decline.
296 At the same time, daily sludge wastage to control the SRT could also remove some dissolved
297 inorganic salts, contributing to a more gradual conductivity increase from day 10 onward
298 (Figure 1). High salinity could negatively affect the system biological stability and membrane
299 performance (Lay et al., 2010). Since salinity build-up continued to occur, a long term study
300 is necessary to determine the steady state level of salinity in the bioreactor. It is also noted
301 that several strategies to mitigate salinity build-up in OMBR have been proposed, for
302 example, by using organic draw solutions (Luo et al., 2016a) and integrating with the MF/UF
303 membrane for salt bleeding (Holloway et al., 2015; Luo et al., 2016b).

304 In contrast to salinity build-up in OMBR, the mixed liquor conductivity was constant at
305 approximately 0.38 mS/cm (corresponding to 0.19 g/L NaCl) throughout conventional MBR
306 operation (Figure 1). This is because the MF membrane does not retain any dissolved salts.
307 Overall, different sludge characteristics, microbial community structure, and biological
308 treatment performance between OMBR and conventional MBR were observed as discussed
309 in the following sections.

310

[Figure 1]

311 A continuous decrease in the water flux was observed for OMBR (Figure 1). The observed
312 flux decline could be ascribed to salinity build-up in the bioreactor, a decrease in the draw
313 solution concentration, and membrane fouling. Although the RO membrane effectively
314 rejected NaCl solute (> 98%), the draw solution concentration decreased over time (Figure S2,
315 Supplementary Data), due to the reverse solute transport and, to a lesser extent, its passage
316 through the RO membrane. Both salinity increase in the bioreactor and concentration
317 decrease of the draw solution could reduce the net driving force (i.e. effective trans-
318 membrane osmotic pressure) for water permeation. On day 20 of the experiment, 100 g NaCl
319 was added to replenish the draw solute loss, which slightly enhanced the water flux (by
320 approximately 1.5 L/m²h). Despite the low fouling propensity of the FO membrane, a cake
321 layer was observed on the membrane surface at the conclusion of OMBR operation,
322 predominately consisting of carbon, oxygen, phosphorus, sodium, magnesium, and calcium
323 (Figure S3, Supplementary Data).

324 Water flux of conventional MBR was adjusted daily to match that of OMBR and thus
325 maintain a comparable effluent flux toward the downstream RO process. As a result, the MF
326 membrane was operated at a relatively low water flux, which in turn resulted in negligible
327 membrane fouling as indicated by a small TMP increase throughout conventional MBR
328 operation (Figure S4, Supplementary Data). In practice, the water flux of conventional MBR
329 is usually above 10 L/m²h (Hai et al., 2014), which is considerably higher than the water flux
330 (4 – 8 L/m²h) used in this study. Although FO is more resistant to fouling compared to
331 UF/MF given the different mechanisms of water transport (i.e. osmotically driven and
332 hydraulic pressure driven for FO and UF/MF, respectively), fouling behaviour and separation
333 performance of FO at a higher flux can differ from those reported here. Nevertheless, with
334 continued progress in membrane development (Fane et al., 2015; Shaffer et al., 2015; Werber

335 et al., 2016), fouling resistant, high flux and high separation performance FO membranes can
336 be available in a near future. Indeed, several different research groups have reported new FO
337 membranes with water permeability two to three times higher than that of the commercial
338 membrane used in this study (Tian et al., 2015; Wei et al., 2015). Such progress in membrane
339 fabrication may provide more opportunities in the deployment of OMBR with better
340 contaminant removal and less membrane fouling.

341 *3.1.2 Biomass characteristics*

342 Salinity build-up in the bioreactor altered biomass characteristics during OMBR operation
343 (Figure 2). A small but discernible decrease in biomass concentration (i.e. MLSS and
344 MLVSS) and SOUR was observed within the first two weeks (Figure 2a-c). This observation
345 is in good agreement with previous studies (Wang et al., 2014; Luo et al., 2015b), and could
346 be ascribed to the inhibition on biomass growth and activity with salinity increase. In
347 addition, the high salinity also increased SMP and EPS concentrations in the mixed liquor
348 (Figure 2d, e), which might be responsible for the FO membrane fouling as discussed above.
349 It has been reported that the elevated salinity could increase the endogenous respiration of
350 microorganisms in activated sludge and thus enhance the secretion of organic cellular
351 substances (Lay et al., 2010; Chen et al., 2014). Nevertheless, biomass concentration and
352 activity recovered gradually from day 14 onward, possibly due to microbial acclimatization
353 to the saline condition, which consequently resulted in the dominance of halotolerant bacteria
354 in the bioreactor (Figures 3 and 4). Meanwhile, SMP and EPS concentrations in the mixed
355 liquor decreased and then stabilized at approximately 20 and 55 mg/g MLVSS, respectively
356 (Figure 2d, e).

357 **[Figure 2]**

358 Biomass growth (indicated by the MLSS and MLVSS concentrations) and activity (indicated
359 by the sludge SOUR) were relatively stable during conventional MBR operation (Figure 2).
360 However, both SMP and EPS concentrations in the mixed liquor decreased significantly,
361 likely due to a reduction in the organic loading rate caused by the decreasing water flux (to
362 match that of OMBR). Given a stable sludge concentration, a decrease in the organic loading
363 rate could lower the ratio of food to microorganism (i.e. F/M), thereby increasing the SMP
364 and EPS biodegradation (Wu et al., 2013).

365 3.1.3 *Microbial community structure*

366 Sludge samples collected from OMBR and conventional MBR were clustered based on the
367 unweighted Unifrac distance by applying hierarchical clustering (Figure 3). The unweighted
368 Unifrac distance among samples represents the dissimilarity in their microbial communities
369 in a phylogenetic tree. Results show that microbial community structure varied differently in
370 OMBR and conventional MBR (Figures 3 and 4). Sludge samples taken at the beginning of
371 OMBR and conventional MBR operation (i.e. on day 0) formed one cluster, confirming
372 similar microbial communities in these two systems at the initial phase (Figure 3). However,
373 the sludge sample collected at the end of OMBR operation (i.e. on day 40) created a branch
374 distinct from the cluster of other samples. This result indicates that salinity build-up in
375 OMBR significantly impacted the development of the microbial community, rendering it
376 different from that in conventional MBR. In addition, distant clusters were observed for the
377 two sludge samples taken at the beginning and conclusion of conventional MBR operation.
378 This observation could be attributed to microbial variation in response to the prolonging HRT
379 due to continuous water flux decline (Figure 1). It is noteworthy that natural and transient
380 changes in microbial community during MBR operation could also occur (Luo et al., 2016c;
381 Phan et al., 2016).

382 **[Figure 3]**

383

[Figure 4]

384 Further taxonomic analysis revealed significant difference in the microbial community
385 between OMBR and conventional MBR (Figure 3). For instance, the phylum *Planctomycetes*
386 in conventional MBR was much more abundant than that in OMBR (Figure 4a). This result is
387 consistent with our previous study that showed a decrease in the abundance of the phylum
388 *Planctomycetes* in a conventional MBR when its influent salinity increased (Luo et al.,
389 2016c). Microbial species of the phylum *Bacteroidetes* are usually detected in both marine
390 and freshwater environments (Zhang et al., 2013). Thus, the phylum *Bacteroidetes* was
391 identified in all sludge samples with noticeable abundance (Figure 4a). Nevertheless, the
392 abundance of the phylum *Bacteroidetes* increased during OMBR operation, which could be
393 further attributed to an increase in the dominance of the family *Cytophagaceae* (Figure 4b).

394 Abundance of the phylum *Proteobacteria* varied differently during OMBR and conventional
395 MBR operation, although it was the most abundant phylum in both systems (Figure 4a). As
396 conventional MBR operated, the abundance of the phylum *Proteobacteria* increased
397 significantly, which was mainly contributed by the dominance of the class *β -proteobacteria*.
398 Members of the class *β -proteobacteria* are typically dominant in freshwater environment
399 (Zhang et al., 2013). Detailed analysis attributed this class dominance to the predominance of
400 the families *Oxalobacteraceae* and *Comamonadaceae* (Figure 4b). By contrast, a small
401 increase in the abundance of the class *β -proteobacteria* was observed during OMBR
402 operation, which was only contributed by the dominance of the family *Comamonadaceae*.
403 Zhang et al. (2013) also reported an increase in the abundance of the class *β -proteobacteria*
404 along a salinity gradient of 0.34 – 6.86 g/L NaCl in a Chinese wetland. These results indicate
405 that some microbes affiliated to the class *β -proteobacteria*, such as *Comamonadaceae*, are
406 salt-tolerant and could proliferate under saline conditions. On the other hand, the abundance
407 of the class *γ -proteobacteria* decreased considerably in both systems mainly due to the

408 decaying of the family *Xanthomonadaceae*. A similar decrease in both systems also occurred
409 for the family *Ellin 6075* belonged to the phylum *Acidobacteria*.

410 3.2 Contaminant removal

411 3.2.1 Removal of bulk organic matter and nutrients

412 No significant difference between OMBR-RO and conventional MBR-RO was observed
413 regarding overall removal of bulk organic matter (i.e. TOC and TN) (Figure 5) and nutrients
414 (i.e. NH_4^+ and PO_4^{3-}) (Figure 6). Nevertheless, these contaminants exhibited considerably
415 different fates and transport behaviours in the two hybrid systems. A small increase in TOC
416 concentration in the bioreactor was observed at the beginning of OMBR operation (Figure
417 5a). This observation could be attributed to negative effects of salinity build-up on biomass
418 activity as discussed above and the high rejection of biologically persistent substances by the
419 FO membrane. The high rejection FO membrane resulted in negligible TOC concentration in
420 the draw solution and thus ensured a complete overall removal by OMBR-RO. Given the
421 stable biological treatment and the permeation of non-biodegradable organic substances
422 through the MF membrane, TOC concentration in the bioreactor during conventional MBR
423 operation was less than one-tenth of that in OMBR (Figure 5b). Organic substances that were
424 resistant to conventional MBR treatment were effectively retained by the RO membrane,
425 causing notable TOC accumulation in the MBR effluent reservoir and near complete removal
426 by the whole system.

427 [Figure 5]

428 Without a denitrification step, TN removal by activated sludge is limited and depends mainly
429 on microbial assimilation (Hai et al., 2014). In OMBR-RO operation, the high rejection FO
430 and RO membranes induced a considerable TN accumulation in the bioreactor and the draw
431 solution, respectively (Figure 5c). It has been reported that contaminants that permeated

432 through the FO membrane but were rejected by the RO membrane could accumulate in the
433 draw solution in closed-loop FO-RO systems (e.g. OMBR-RO), and eventually deteriorated
434 the product water quality (Shaffer et al., 2012; D'Haese et al., 2013). As a result, the overall
435 TN removal by OMBR-RO decreased from nearly 100 to 50% within 40 days (Figure 5c). By
436 contrast, TN concentration in the bioreactor was stable at approximately 30 mg/L during
437 conventional MBR operation (Figure 5d). Nevertheless, the high rejection RO membrane
438 caused a significant TN build-up in the MBR effluent reservoir, which consequently reduced
439 its overall removal by MBR-RO (from approximately 98 to 40%).

440 Effective nitrification occurred in both OMBR and conventional MBR systems as manifested
441 by the removal of NH_4^+ in their bioreactors (Figure 6a, b). Nevertheless, ammonia oxidizing
442 bacteria (AOB), which oxidize ammonia to nitrite, were not efficiently detected in all sludge
443 samples (Figure 4). Only nitrite oxidizing bacteria (which oxidize nitrite to nitrate) affiliated
444 to the phylum *Nitrospirae* were identified at a small abundance (Figure 4a). Similar results
445 were also reported previously and could be attributed to the presence of AOB species that
446 were unidentifiable by 16S rRNA-gene sequencing (Luo et al., 2016c; Phan et al., 2016).
447 Additionally, the effective NH_4^+ removal could also be contributed by ammonia oxidizing
448 archaea, which however, were not targeted by the primers designed in this study.

449 **[Figure 6]**

450 Similar to bulk organic matter (i.e. TOC), a small and transient increase in NH_4^+
451 concentration was observed in the bioreactor at the beginning of OMBR operation (Figure
452 6a). Nevertheless, the high rejection FO membrane resulted in negligible NH_4^+ concentration
453 in the draw solution. On the other hand, NH_4^+ concentration in the bioreactor was constantly
454 low during conventional MBR operation. However, the high rejection RO membrane induced
455 a small but discernible NH_4^+ build-up in the MBR effluent reservoir from day 20 onward.

456 Without chemical precipitation, phosphate removal in activated sludge treatment relies
457 mainly on microbial assimilation, especially by polyphosphate accumulating organisms
458 (PAOs). PAOs are vulnerable to saline stress and a small osmotic pressure increase within
459 their cells caused by salinity build-up may severely reduce their phosphate accumulating
460 ability (Lay et al., 2010; Yogalakshmi, 2010). Nevertheless, the FO membrane can almost
461 completely retain phosphate ions as they are negatively charged and have large hydrated
462 radius (Holloway et al., 2007). As a result, PO_4^{3-} accumulated considerably in the bioreactor
463 while its presence in the draw solution was negligible during OMBR-RO operation (Figure
464 6c). On the other hand, phosphate could permeate through the MF but not the RO membrane.
465 Thus, phosphate build-up in the MBR effluent reservoir was observed during conventional
466 MBR-RO operation (Figure 6d). It is noteworthy that PO_4^{3-} concentration in the bioreactor
467 was slightly higher than that in influent during conventional MBR operation, possibly owing
468 to its retention by the dynamic fouling layer formed on the MF membrane surface and/or
469 phosphate release from unmetabolized substrates (Yogalakshmi, 2010).

470 3.2.2 Removal of trace organic contaminants

471 All 31 TrOCs investigated were almost completely removed by both OMBR-RO and
472 conventional MBR-RO (Figure 6), due to the synergy of biological treatment and physical
473 membrane rejection. Nevertheless, removal behaviours of these TrOCs were significantly
474 different in these two hybrid systems, depending on their physiochemical properties,
475 including hydrophobicity and molecular structure (Table S1, Supplementary Data). Of the 31
476 TrOCs investigated, 18 compounds were hydrophilic (i.e. $\text{Log } D < 3.2$) and 13 compounds
477 were hydrophobic (i.e. $\text{Log } D > 3.2$) (Section 2.1).

478 **[Figure 7]**

479 All 13 hydrophobic TrOCs were biologically removed by over 90% in both systems (Figure
480 7). Compared to conventional MBR, salinity build-up in the bioreactor did not significantly
481 affect the biological removal of these hydrophobic compounds during OMBR operation.
482 Their high removal by activated sludge has also been demonstrated in several previous
483 studies (Tadkaew et al., 2011; Wijekoon et al., 2013) and can be ascribed to their adsorption
484 onto sludge, which facilitated their biodegradation. Results reported here are also consistent
485 with a previous study by Luo et al. (2015b) who reported insignificant variation in the
486 removal of hydrophobic TrOCs by conventional MBR as the mixed liquor salinity increased
487 (up to 16.5 g/L NaCl). The effective removal of hydrophobic TrOCs by activated sludge
488 could consequently reduce their permeation through the FO and subsequent RO membranes,
489 leading to near complete removal by both hybrid systems (Figure 7). It has been reported that
490 an initial adsorption but subsequent partition and diffusion of hydrophobic TrOCs
491 (particularly, non-ionic compounds) through membranes could reduce their rejection in a
492 stand-alone FO or RO process (Nghiem and Coleman, 2008; Xie et al., 2014).

493 Varying removal rates of hydrophilic TrOCs were observed in both bioreactors (Figure 7).
494 Effective removal (> 90%) was observed for several hydrophilic compounds, including
495 salicylic acid, ketoprofen, naproxen, metronidazole, ibuprofen, gemfibrozil, enterolactone,
496 pentachlorophenol, DEET, and estriol. This result can be attributed to the high
497 biodegradability of these compounds, whose molecular structures have strong electron
498 donating functional groups (e.g. amine and hydroxyl) (Tadkaew et al., 2011). On the other
499 hand, some hydrophilic TrOCs were poorly removed in both bioreactors, with removal rates
500 only in the range of 20 – 70%. They included clofibric acid, fenprop, primidone, diclofenac,
501 carbamazepine, atrazine, and ametryn, which are well-known biologically resistant
502 substrates. Their resistance to biological treatment mainly resulted from the presence of
503 strong electron withdrawing functional groups (such as chloride, amide, and nitro) or the lack

504 of strong electron donating functional groups in their molecular structures (Tadkaew et al.,
505 2011; Wijekoon et al., 2013).

506 Despite the low removal of biologically persistent TrOCs by activated sludge, the high
507 rejection FO membrane prevented their permeation into the draw solution and allowed almost
508 complete removal by OMBR (Figure 7a). A small but nevertheless discernible contribution
509 by the downstream RO membrane was only observed for atrazine and ametryn, which were
510 slightly permeable through the FO membrane. Our results are consistent with previous
511 studies which demonstrated excellent removal of TrOCs by FO or FO-RO (Hancock et al.,
512 2011; D'Haese et al., 2013; Alturki et al., 2013). On the other hand, conventional MBR could
513 not effectively remove these biologically persistent TrOCs although the dynamic fouling
514 layer formed on the MF membrane surface rejected them to some extent (Figure 7b).
515 Nevertheless, the high rejection RO membrane complemented well to MBR for the high
516 overall removal of these compounds.

517 3.3 Reverse osmosis membrane fouling

518 Water flux of the RO process subsequent to conventional MBR was adjusted daily to match
519 that of the RO process subsequent to OMBR (Section 2.3). Changes in the applied hydraulic
520 pressures to the RO membrane in these two hybrid systems are shown in Figure 8a. To
521 compare fouling development on the RO membrane surface, the normalized water
522 permeability was also determined (Figure 8b), which is the ratio of the effective membrane
523 water permeability to the initial value (P/P_0).

524 **[Figure 8]**

525 The normalized water permeability of the RO membrane decreased less significantly than in
526 conventional MBR-RO (Figure 8). This result indicates that the RO membrane fouling was
527 more severe when treating conventional MBR effluent compared to reconcentrating the

528 OMBR draw solution due to their different water qualities and foulant contents (Figures 5
529 and 6). Thus, although the RO membrane in OMBR-RO was operated at a higher initial
530 hydraulic pressure to overcome the osmotic pressure of the draw solution (i.e. 0.5 M NaCl),
531 the hydraulic pressure applied to the RO membrane in conventional MBR-RO increased
532 much more rapidly and frequent RO membrane replacement was needed to match the water
533 flux of OMBR-RO (Figure 8a). Severe RO membrane fouling observed in conventional
534 MBR-RO can be attributed to foulant accumulation in the MBR effluent reservoir. Indeed,
535 EEM analysis revealed foulant build-up, such as humic-like ($\lambda_{ex/em}=300-370/400-500$ nm)
536 and protein-like substances ($\lambda_{ex/em}=275-290/330-370$ nm), in the MBR effluent (Figure S5,
537 Supplementary Data).

538 The FO process effectively prevented foulants from permeating into the draw solution
539 (Figures 6 and 7), thereby reducing membrane fouling in the downstream RO process. For
540 instance, the humic- and protein-like substances accumulated considerably in the bioreactor,
541 but their presence in the draw solution was negligible (Figure S5, Supplementary Data).
542 However, the RO normalized water permeability decreased gradually and stabilized at
543 approximately 0.35 from day 20 onward during OMBR-RO operation (Figure 8b). The
544 observed permeability decline could be attributed to membrane compaction (particularly
545 within the first week of operation) and fouling under the high hydraulic pressure (Figure 8a).
546 The fouling layer on the RO membrane surface exhibited different morphologies in OMBR-
547 RO and conventional MBR-RO (Figure 9a, b). Foulant clusters were sparsely distributed
548 without forming a dense fouling layer on the RO membrane surface subsequent to OMBR
549 (Figure 9a). Elementary analysis by EDS revealed that these clusters comprised carbon,
550 oxygen, sodium, and chloride (Figure 9c). By contrast, a compact and homogenous cake
551 layer formed on the RO membrane surface in conventional MBR-RO (Figure 9b),
552 predominantly containing carbon, oxygen, magnesium, calcium, and phosphate (Figure 9d).

553 This result indicates the formation of both organic and inorganic membrane fouling. However,
554 regularly shaped or needle-like crystals typically formed with inorganic scaling were not
555 visualized on the RO membrane surface subsequent to conventional MBR although
556 magnesium, calcium, and phosphate were detected (Figure 9b). This result was possibly due
557 to the formation of inorganic precipitates in the organic fouling layer or the complexation
558 between these divalent cations and organic molecules (e.g. protein-like substances) on the
559 membrane surface (Zhao et al., 2010).

560 **[Figure 9]**

561 Organic fouling layer on the RO membrane surface was characterized by ATR-FTIR
562 measurement (Figure 10). The pristine RO membrane showed typical absorbance peaks at
563 wavenumbers of 3345 cm^{-1} (N-H stretching), 3300 cm^{-1} (O-H stretching), 1671 cm^{-1} (strong
564 amide C=O), 2946 and 1487 cm^{-1} (C-H stretching), and 1168 cm^{-1} (amide ring). Similar ATR-
565 FTIR spectra were also observed for the RO membrane coupled with OMBR, confirming the
566 formation of slight and scattered organic fouling layer on the membrane surface. By contrast,
567 the RO membrane subsequent to conventional MBR exhibited distinctive adsorption peaks at
568 1653 cm^{-1} , which usually associates with alkene (C=C) in aliphatic structures and/or amide I
569 (C=O) bonds, and at 1543 cm^{-1} , representing amide II (C-N-H) bonds. In addition, the fouled
570 RO membrane also showed a sharp peak at 1032 cm^{-1} , indicating carbonyl (C=O) bonds of
571 polysaccharides. These results suggest that humic- and protein-like substances accumulated
572 in the MBR effluent were likely responsible for the severe organic fouling of the RO
573 membrane in conventional MBR-RO.

574 **[Figure 10]**

575 3.4 Implications

576 High product water quality and low membrane fouling imply robustness of OMBR-RO in
577 advanced wastewater treatment and water reuse. Results reported here highlight the benefits
578 of OMBR-RO over conventional MBR-RO. Compared to conventional MBR-RO, the high
579 rejection FO membrane prevents the downstream RO process from severe membrane fouling,
580 thereby reducing membrane cleaning and maintenance during OMBR-RO operation.
581 Moreover, OMBR-RO has the potential to simultaneously achieve seawater desalination and
582 wastewater recycling when seawater is used as the draw solution in coastal regions. By virtue
583 of osmotic dilution, low pressure RO systems can be coupled with OMBR to remove the need
584 for concentrate disposal, thereby reducing energy consumption for seawater desalination and
585 wastewater recovery (Valladares Linares et al., 2016). several strategies to mitigate salinity
586 build-up in OMBR have been proposed, for example, by using organic draw solutions (Luo et
587 al., 2016a) and integrating with the MF/UF membrane for salt bleeding (Holloway et al.,
588 2015; Luo et al., 2016b).

589 Sludge produced by OMBR is expected to be saline. Thus, further study is necessary to
590 quantify the impact of salinity on subsequent sludge treatment and available sludge reuse
591 options.

592 4. Conclusion

593 Results reported here show that both OMBR-RO and conventional MBR-RO systems can
594 effectively remove bulk organic matter, nutrients, and all 31 TrOCs investigated.
595 Nevertheless, salinity build-up in the bioreactor reduced the water flux and adversely
596 impacted biological stability by altering biomass characteristics and microbial community
597 structure during OMBR operation. Salinity increase also resulted in more SMP and EPS in
598 the mixed liquor, inducing the FO membrane fouling. With the succession of halophobic

599 bacteria by halotolerant ones, the OMBR system remained biologically active. Moreover, the
600 high rejection of foulants by the FO membrane prevented the downstream RO process from
601 severe membrane fouling. In contrast to biological variation in OMBR, biological
602 performance was relatively stable during conventional MBR operation. However, foulants
603 (e.g. humic- and protein-like matters and inorganic salts) accumulated considerably in the
604 MBR effluent reservoir, resulting in severe fouling to the subsequent RO membrane.

605 **5. References**

606 Achilli, A., Cath, T.Y., Marchand, E.A., Childress, A.E., 2009. The forward osmosis
607 membrane bioreactor: A low fouling alternative to MBR processes. *Desalination* 239, 10-
608 21.

609 Al Ashhab, A., Herzberg, M., Gillor, O., 2014. Biofouling of reverse-osmosis membranes
610 during tertiary wastewater desalination: Microbial community composition. *Water Res.*
611 50, 341-349.

612 Alturki, A.A., McDonald, J., Khan, S.J., Hai, F.I., Price, W.E., Nghiem, L.D., 2012.
613 Performance of a novel osmotic membrane bioreactor (OMBR) system: Flux stability and
614 removal of trace organics. *Bioresour. Technol.* 113, 201-206.

615 Alturki, A.A., McDonald, J.A., Khan, S.J., Price, W.E., Nghiem, L.D., Elimelech, M., 2013.
616 Removal of trace organic contaminants by the forward osmosis process. *Sep. Purif.*
617 *Technol.* 103, 258-266.

618 Alturki, A.A., Tadkaew, N., McDonald, J.A., Khan, S.J., Price, W.E., Nghiem, L.D., 2010.
619 Combining MBR and NF/RO membrane filtration for the removal of trace organics in
620 indirect potable water reuse applications. *J. Membr. Sci.* 365, 206-215.

621 APHA. 2005. Standard methods for the examination of water and wastewater. APHA-
622 AWWA-WEF. 9780875530475, 0875530478.

623 Caporaso, J.G., Kuczynski, J., Stombaugh, J., Bittinger, K., Bushman, F.D., Costello, E.K.,
624 Fierer, N., Peña, A.G., Goodrich, J.K., Gordon, J.I., Huttley, G.A., Kelley, S.T., Knights,
625 D., Koenig, J.E., Ley, R.E., Lozupone, C.A., McDonald, D., Muegge, B.D., Pirrung, M.,
626 Reeder, J., Sevinsky, J.R., Turnbaugh, P.J., Walters, W.A., Widmann, J., Yatsunenko, T.,
627 Zaneveld, J., Knight, R., 2010. QIIME allows analysis of high-throughput community
628 sequencing data. *Nat. Methods* 7, 335-336.

629 Cath, T.Y., Hancock, N.T., Lampi, J., Nghiem, L.D., Xie, M., Yip, N.Y., Elimelech, M.,
630 McCutcheon, J.R., McGinnis, R.L., Achilli, A., Anastasio, D., Brady, A.R., Childress,
631 A.E., Farr, I.V., 2013. Standard methodology for evaluating membrane performance in
632 osmotically driven membrane processes. *Desalination* 312, 31-38.

633 Chen, L., Gu, Y., Cao, C., Zhang, J., Ng, J.-W., Tang, C., 2014. Performance of a submerged
634 anaerobic membrane bioreactor with forward osmosis membrane for low-strength
635 wastewater treatment. *Water Res.* 50, 114-123.

636 Clara, M., Strenn, B., Gans, O., Martinez, E., Kreuzinger, N., Kroiss, H., 2005. Removal of
637 selected pharmaceuticals, fragrances and endocrine disrupting compounds in a membrane
638 bioreactor and conventional wastewater treatment plants. *Water Res.* 39, 4797-4807.

639 Cornelissen, E.R., Harmsen, D., Beerendonk, E.F., Qin, J.J., Oo, H., De Korte, K.F.,
640 Kappelhof, J.W.M.N., 2011. The innovative osmotic membrane bioreactor (OMBR) for
641 reuse of wastewater. *Water Sci. Technol.* 63, 1557-1565.

642 Cory, R.M., McKnight, D.M., 2005. Fluorescence spectroscopy reveals ubiquitous presence
643 of oxidized and reduced quinones in dissolved organic matter. *Environ. Sci. Technol.* 39,
644 8142-8149.

645 D'Haese, A., Le-Clech, P., Van Nevel, S., Verbeken, K., Cornelissen, E.R., Khan, S.J.,
646 Verliefe, A.R.D., 2013. Trace organic solutes in closed-loop forward osmosis

647 applications: Influence of membrane fouling and modeling of solute build-up. *Water Res.*
648 47, 5232-5244.

649 De Wever, H., Weiss, S., Reemtsma, T., Vereecken, J., Müller, J., Knepper, T., Rörden, O.,
650 Gonzalez, S., Barcelo, D., Dolores Hernando, M., 2007. Comparison of sulfonated and
651 other micropollutants removal in membrane bioreactor and conventional wastewater
652 treatment. *Water Res.* 41, 935-945.

653 Edgar, R.C., 2013. UPARSE: Highly accurate OTU sequences from microbial amplicon
654 reads. *Nat. Methods* 10, 996-998.

655 Elimelech, M., Phillip, W.A., 2011. The future of seawater desalination: Energy, technology,
656 and the environment. *Science* 333, 712-717.

657 Fane, A.G., Wang, R., Hu, M.X., 2015. *Synthetic Membranes for Water Purification: Status*
658 *and Future. Angew. Chem. Int. Ed.*

659 Farias, E.L., Howe, K.J., Thomson, B.M., 2014. Effect of membrane bioreactor solids
660 retention time on reverse osmosis membrane fouling for wastewater reuse. *Water Res.* 49,
661 53-61.

662 Gerrity, D., Pecson, B., Trussell, R.S., Trussell, R.R., 2013. Potable reuse treatment trains
663 throughout the world. *J. Water Supply Res. Technol. AQUA* 62, 321-338.

664 Hai, F.I., Tessmer, K., Nguyen, L.N., Kang, J., Price, W.E., Nghiem, L.D., 2011. Removal of
665 micropollutants by membrane bioreactor under temperature variation. *J. Membr. Sci.* 383,
666 144-151.

667 Hai, F.I., Yamamoto, K., Lee, C.H. 2014. *Membrane Biological Reactors: Theory, Modeling,*
668 *Design, Management and Applications to Wastewater Reuse. IWA Publishing, London.*

669 Hancock, N.T., Xu, P., Heil, D.M., Bellona, C., Cath, T.Y., 2011. Comprehensive bench- and
670 pilot-scale investigation of trace organic compounds rejection by forward osmosis.
671 *Environ. Sci. Technol.* 45, 8483-8490.

672 Henderson, R.K., Baker, A., Murphy, K.R., Hambly, A., Stuetz, R.M., Khan, S.J., 2009.
673 Fluorescence as a potential monitoring tool for recycled water systems: A review. *Water*
674 *Research* 43, 863-881.

675 Holloway, R.W., Childress, A.E., Dennett, K.E., Cath, T.Y., 2007. Forward osmosis for
676 concentration of anaerobic digester centrate. *Water Res.* 41, 4005-4014.

677 Holloway, R.W., Regnery, J., Nghiem, L.D., Cath, T.Y., 2014. Removal of trace organic
678 chemicals and performance of a novel hybrid ultrafiltration-osmotic membrane
679 bioreactor. *Environ. Sci. Technol.* 48, 10859-10868.

680 Holloway, R.W., Wait, A.S., Da Silva, A.F., Herron, J., Schutter, M.D., Lampi, K., Cath,
681 T.Y., 2015. Long-term pilot scale investigation of novel hybrid ultrafiltration-osmotic
682 membrane bioreactors. *Desalination* 363, 64.

683 Kim, Y., Elimelech, M., Shon, H.K., Hong, S., 2014. Combined organic and colloidal fouling
684 in forward osmosis: Fouling reversibility and the role of applied pressure. *J. Membr. Sci.*
685 460, 206-212.

686 Lay, W.C.L., Liu, Y., Fane, A.G., 2010. Impacts of salinity on the performance of high
687 retention membrane bioreactors for water reclamation: A review. *Water Res.* 44, 21-40.

688 Lu, X., Ma, J., Nejati, S., Choo, Y., Osuji, C.O., Elimelech, M., 2015. Elements provide a
689 clue: Nanoscale characterization of thin-film composite polyamide membranes. *ACS*
690 *Appl. Mater. Interfaces* 7, 16917-16922.

691 Luo, W., Hai, F.I., Price, W.E., Elimelech, M., Nghiem, L.D., 2016a. Evaluating ionic
692 organic draw solutes in osmotic membrane bioreactors for water reuse. *J. Membr. Sci.*
693 514, 636-645.

694 Luo, W., Hai, F.I., Price, W.E., Guo, W., Ngo, H.H., Yamamoto, K., Nghiem, L.D., 2014a.
695 High retention membrane bioreactors: Challenges and opportunities. *Bioresour. Technol.*
696 167, 539-546.

697 Luo, W., Hai, F.I., Price, W.E., Guo, W., Ngo, H.H., Yamamoto, K., Nghiem, L.D., 2016b.
698 Phosphorus and water recovery by a novel osmotic membrane bioreactor–reverse osmosis
699 system. *Bioresour. Technol.* 200, 297-304.

700 Luo, W., Hai, F.I., Price, W.E., Nghiem, L.D., 2015a. Water extraction from mixed liquor of
701 an aerobic bioreactor by forward osmosis: Membrane fouling and biomass characteristics
702 assessment. *Sep. Purif. Technol.* 145, 56-62.

703 Luo, W., Phan, H.V., Hai, F.I., Price, W.E., Guo, W., Ngo, H.H., Yamamoto, K., Nghiem,
704 L.D., 2016c. Effects of salinity build-up on the performance and bacterial community
705 structure of a membrane bioreactor. *Bioresour. Technol.* 200, 305-310.

706 Luo, W.H., Hai, F.I., Kang, J.G., Price, W.E., Guo, W.S., Ngo, H.H., Yamamoto, K.,
707 Nghiem, L.D., 2015b. Effects of salinity build-up on biomass characteristics and trace
708 organic chemical removal: Implications on the development of high retention membrane
709 bioreactors. *Bioresour. Technol.* 177, 274-281.

710 Luo, Y.L., Guo, W.S., Ngo, H.H., Nghiem, L.D., Hai, F.I., Zhang, J., Liang, S., Wang,
711 X.C.C., 2014b. A review on the occurrence of micropollutants in the aquatic environment
712 and their fate and removal during wastewater treatment. *Sci. Total Environ.* 473, 619-641.

713 Mi, B., Elimelech, M., 2010. Organic fouling of forward osmosis membranes: Fouling
714 reversibility and cleaning without chemical reagents. *J. Membr. Sci.* 348, 337-345.

715 Nghiem, L.D., Coleman, P.J., 2008. NF/RO filtration of the hydrophobic ionogenic
716 compound triclosan: Transport mechanisms and the influence of membrane fouling. *Sep.*
717 *Purif. Technol.* 62, 709-716.

718 Nguyen, L.N., Hai, F.I., Kang, J., Price, W.E., Nghiem, L.D., 2013. Removal of emerging
719 trace organic contaminants by MBR-based hybrid treatment processes. *Int. Biodeterior.*
720 *Biodegrad.* 85, 474-482.

721 Nguyen, N.C., Chen, S.-S., Nguyen, H.T., Ray, S.S., Ngo, H.H., Guo, W., Lin, P.-H., 2016.
722 Innovative sponge-based moving bed–osmotic membrane bioreactor hybrid system using
723 a new class of draw solution for municipal wastewater treatment. *Water Res.* 91, 305-313.

724 Phan, H.V., Hai, F.I., Zhang, R., Kang, J., Price, W.E., Nghiem, L.D., 2016. Bacterial
725 community dynamics in an anoxic-aerobic membrane bioreactor – Impact on nutrient and
726 trace organic contaminant removal. *Int. Biodeterior. Biodegrad.* 109, 61-72.

727 Semblante, G.U., Hai, F.I., Bustamante, H., Guevara, N., Price, W.E., Nghiem, L.D., 2015.
728 Effects of iron salt addition on biosolids reduction by oxic-settling-anoxic (OSA) process.
729 *Int. Biodeterior. Biodegrad.* 104, 391-400.

730 Shaffer, D.L., Werber, J.R., Jaramillo, H., Lin, S., Elimelech, M., 2015. Forward osmosis:
731 Where are we now? *Desalination* 356, 271-284.

732 Shaffer, D.L., Yip, N.Y., Gilron, J., Elimelech, M., 2012. Seawater desalination for
733 agriculture by integrated forward and reverse osmosis: Improved product water quality for
734 potentially less energy. *J. Membr. Sci.* 415-416, 1-8.

735 Tadkaew, N., Hai, F.I., McDonald, J.A., Khan, S.J., Nghiem, L.D., 2011. Removal of trace
736 organics by MBR treatment: The role of molecular properties. *Water Res.* 45, 2439-2451.

737 Tian, M., Wang, Y.-N., Wang, R., 2015. Synthesis and characterization of novel high-
738 performance thin film nanocomposite (TFN) FO membranes with nanofibrous substrate
739 reinforced by functionalized carbon nanotubes. *Desalination* 370, 79-86.

740 Valladares Linares, R., Li, Z., Yangali-Quintanilla, V., Ghaffour, N., Amy, G., Leiknes, T.,
741 Vrouwenvelder, J.S., 2016. Life cycle cost of a hybrid forward osmosis – low pressure
742 reverse osmosis system for seawater desalination and wastewater recovery. *Water Res.*
743 88, 225-234.

744 Wang, X.H., Yuan, B., Chen, Y., Li, X.F., Ren, Y.P., 2014. Integration of micro-filtration
745 into osmotic membrane bioreactors to prevent salinity build-up. *Bioresour. Technol.* 167,
746 116-123.

747 Wei, R., Zhang, S., Cui, Y., Ong, R.C., Chung, T.-S., Helmer, B.J., de Wit, J.S., 2015. Highly
748 permeable forward osmosis (FO) membranes for high osmotic pressure but viscous draw
749 solutes. *J. Membr. Sci.* 496, 132-141.

750 Werber, J.R., Osuji, C.O., Elimelech, M., 2016. Materials for next-generation desalination
751 and water purification membranes. *Nat. Rev. Mater.* 1, 16018.

752 Wijekoon, K.C., Hai, F.I., Kang, J., Price, W.E., Guo, W., Ngo, H.H., Nghiem, L.D., 2013.
753 The fate of pharmaceuticals, steroid hormones, phytoestrogens, UV-filters and pesticides
754 during MBR treatment. *Bioresour. Technol.* 144, 247-254.

755 Wu, B., Kitade, T., Chong, T.H., Lee, J.Y., Uemura, T., Fane, A.G., 2013. Flux-dependent
756 fouling phenomena in membrane bioreactors under different food to microorganisms
757 (F/M) ratios. *Sep. Sci. Technol.* 48, 840-848.

758 Xie, M., Gray, S.R., 2016. Transport and accumulation of organic matter in forward osmosis-
759 reverse osmosis hybrid system: Mechanism and implications. *Sep. Purif. Technol.* 167, 6-
760 16.

761 Xie, M., Lee, J., Elimelech, M., Nghiem, L.D., 2015. Role of pressure in organic fouling in
762 forward osmosis and reverse osmosis. *J. Membr. Sci.* 493, 748-754.

763 Xie, M., Nghiem, L.D., Price, W.E., Elimelech, M., 2014. Relating rejection of trace organic
764 contaminants to membrane properties in forward osmosis: Measurements, modelling and
765 implications. *Water Res.* 49, 265-274.

766 Yogalakshmi, K.N., 2010. Effect of transient sodium chloride shock loads on the
767 performance of submerged membrane bioreactor. *Bioresour. Technol.* 101, 7054-7061.

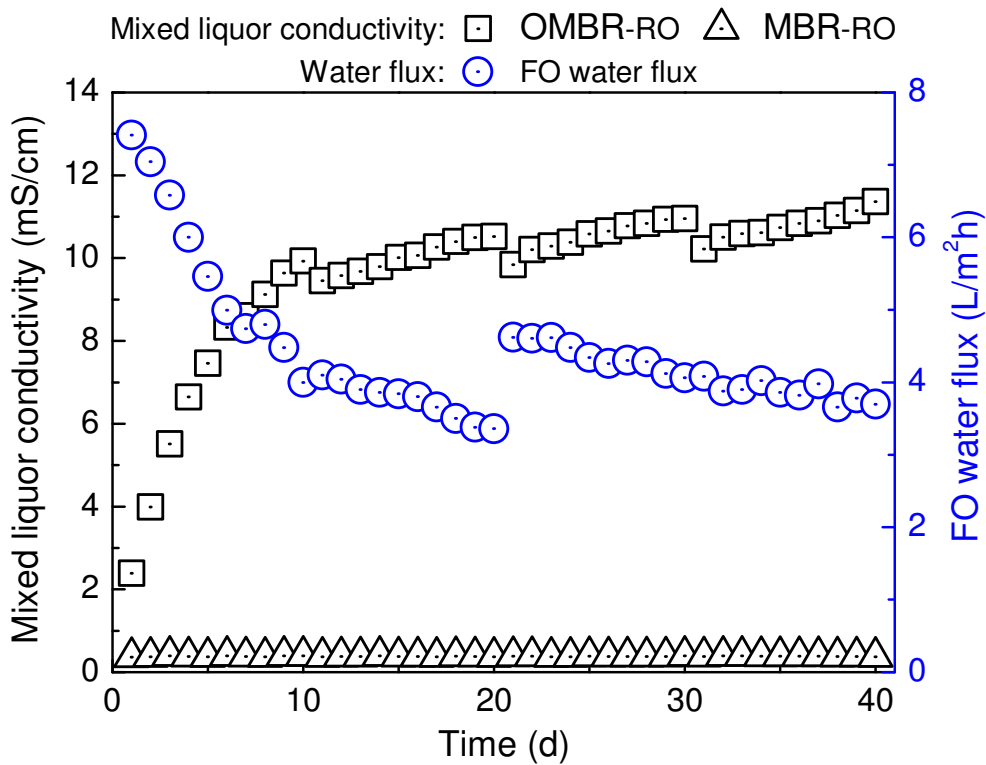
768 Zhang, J.J., Kobert, K., Flouri, T., Stamatakis, A., 2014. PEAR: a fast and accurate Illumina
769 Paired-End reAd mergeR. *Bioinformatics* 30, 614-620.

770 Zhang, L., Gao, G., Tang, X., Shao, K., Bayartu, S., Dai, J., 2013. Bacterial community
771 changes along a salinity gradient in a Chinese wetland. *Can. J. Microbiol.* 59, 611-619.

772 Zhang, X., Bishop, P.L., Kinkle, B.K., 1999. Comparison of extraction methods for
773 quantifying extracellular polymers in biofilms. *Water Sci. Technol.* 39, 211-218.

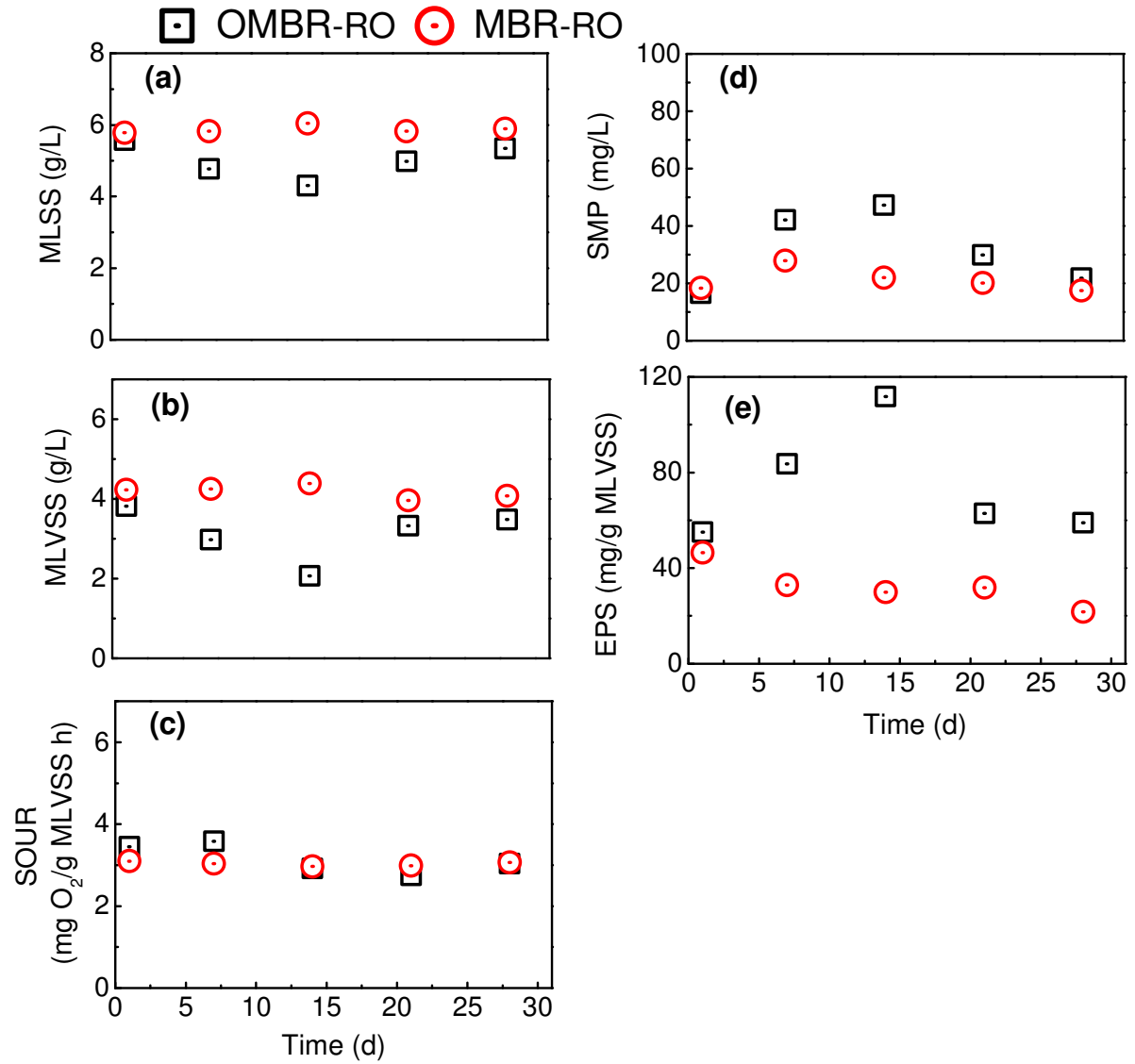
774 Zhao, Y., Song, L., Ong, S.L., 2010. Fouling behavior and foulant characteristics of reverse
775 osmosis membranes for treated secondary effluent reclamation. *J. Membr. Sci.* 349, 65-
776 74.

777 **LIST OF FIGURES**



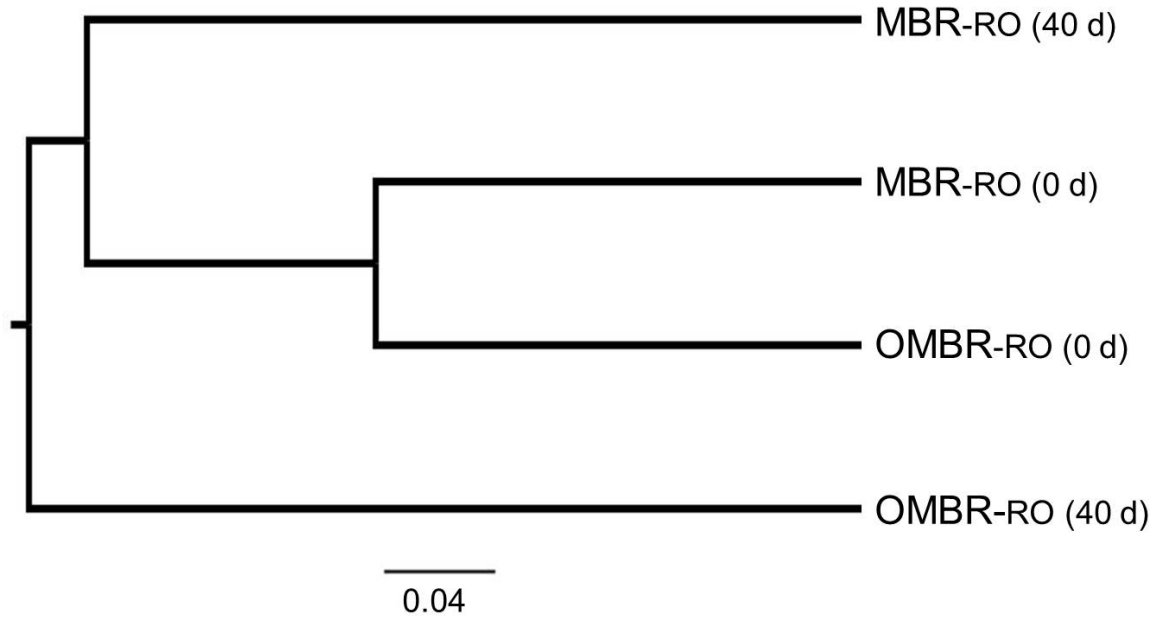
778

779 **Figure 1:** Mixed liquor electrical conductivity and FO water flux during OMBR-RO and
 780 conventional MBR-RO operation. MF (used in conventional MBR) and RO water fluxes
 781 were adjusted daily to match that of FO. The MF membrane was operated in a cycle of 14
 782 min on and 1 min off. Experimental conditions: DO = 5 mg/L; initial MLSS = 5.5 g/L; HRT
 783 = 27 – 60 h; SRT = 20 d; temperature = 22 ± 1 °C; initial FO draw solution = 0.5 M NaCl;
 784 draw cross-flow velocity = 2.8 cm/s; RO cross-flow velocity = 41.5 cm/s. On day 20, 100 g
 785 NaCl was added to OMBR draw solution (with constant working volume of 10 L) to
 786 replenish draw solute loss.



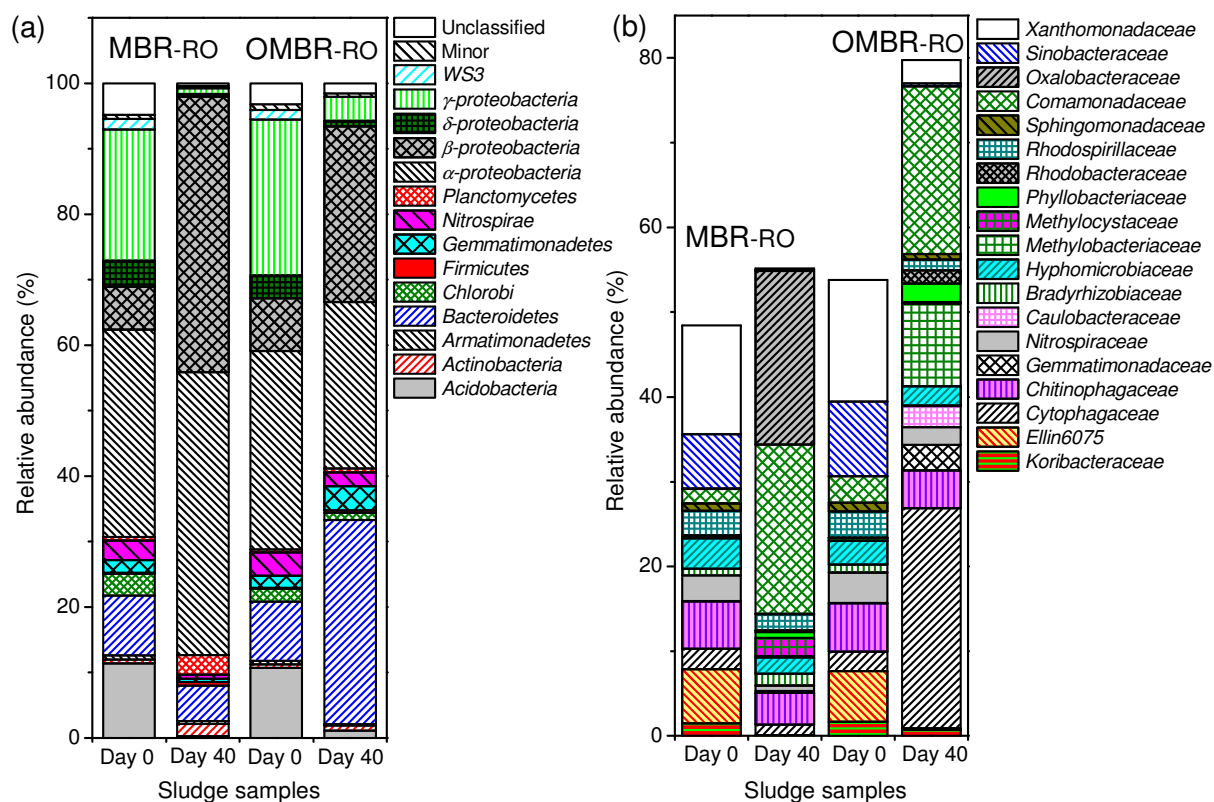
787

788 **Figure 2:** Key biomass characteristics during OMBR-RO and conventional MBR-RO
 789 operation.



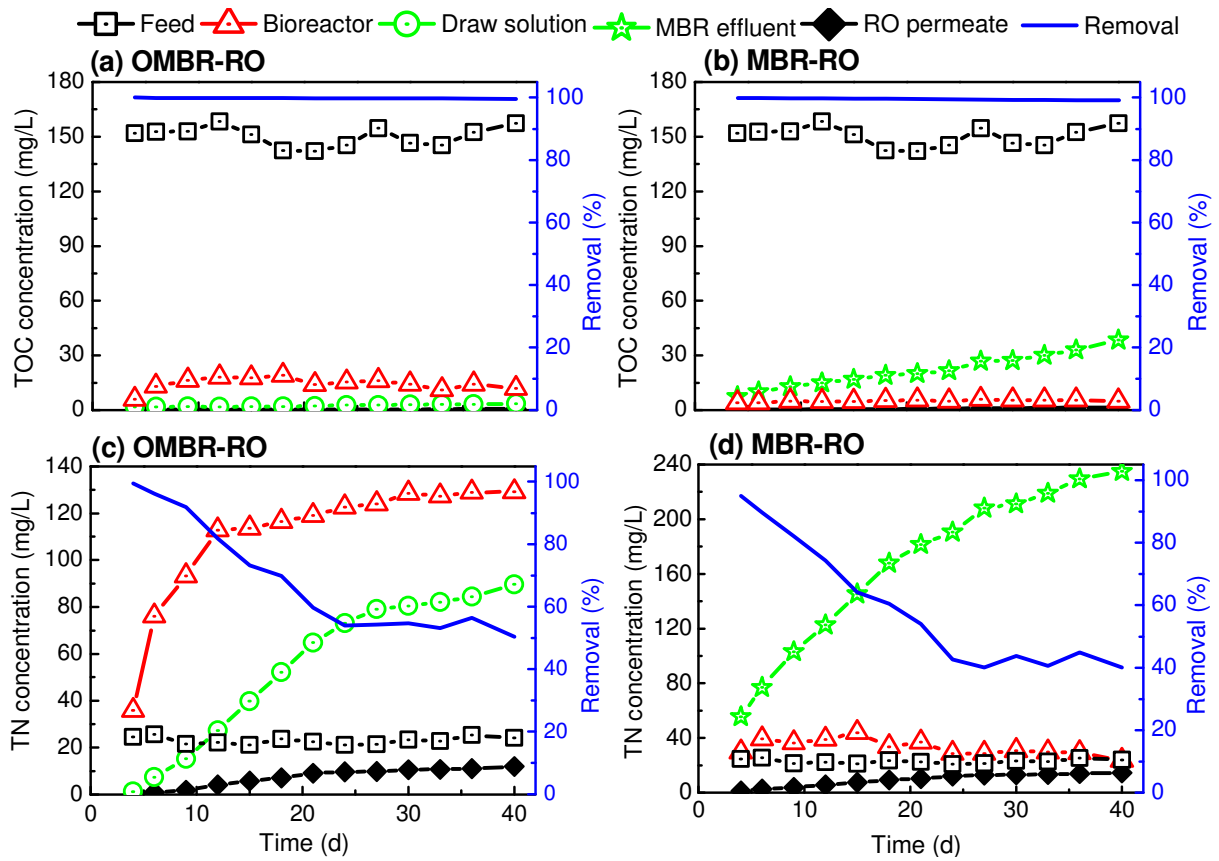
790

791 **Figure 3:** Hierarchical clustering based on the unweighted UniFrac metric. The branch length
 792 represents the distance (indicated by scale bar) among bacterial communities of sludge
 793 samples in UniFrac units. Labels on the branch indicate sludge samples collected from
 794 bioreactors at the beginning (0 day) and conclusion (40 day) of OMBR-RO and conventional
 795 MBR-RO operation. Experimental conditions are as described in the caption of Figure 1.



797

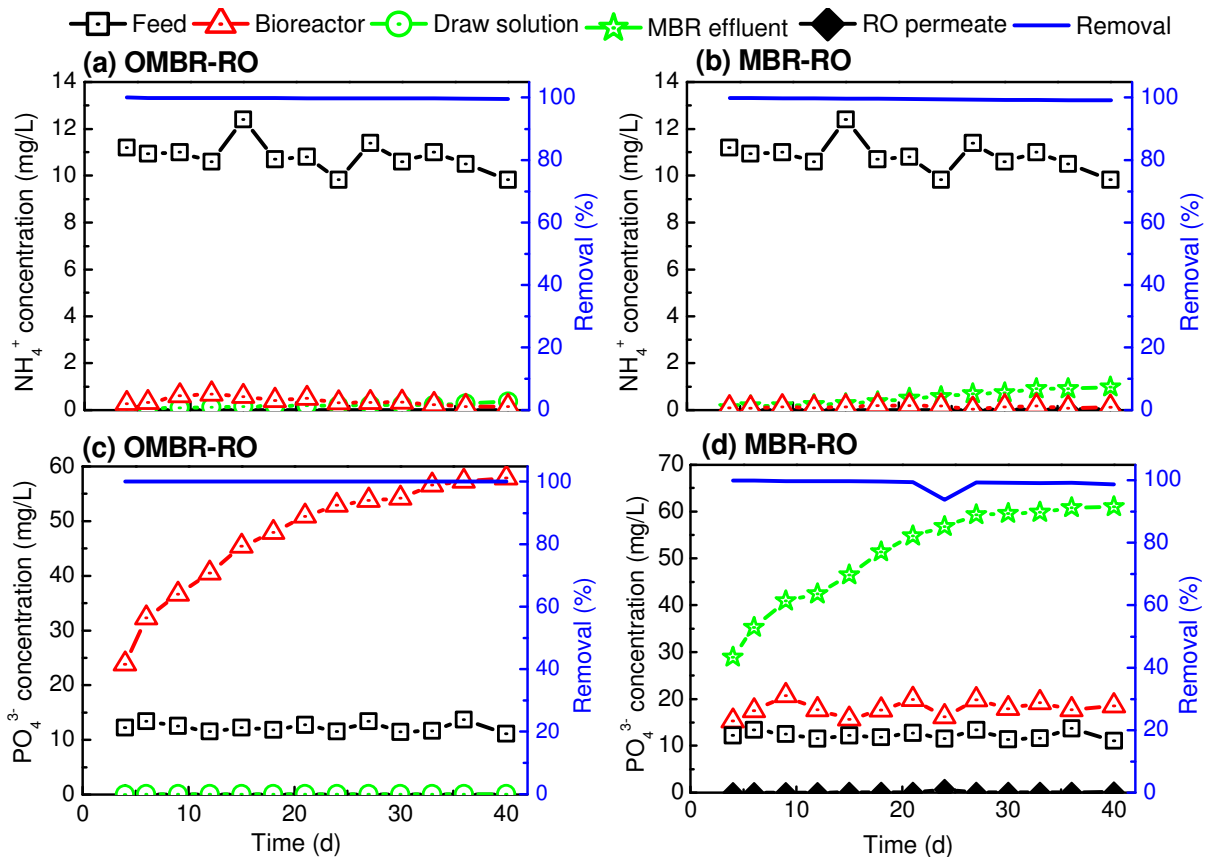
798 **Figure 4:** Relative abundance of dominant (a) phyla and (b) families (>1%) in sludge
 799 samples collected from bioreactors at the beginning (day 0) and conclusion (day 40) of
 800 OMBR-RO and conventional MBR-RO operation. The phylum *Proteobacteria* comprised the
 801 classes α -, β -, δ - and γ -*proteobacteria*. Phyla with relative abundance < 0.5% were grouped
 802 as “Minor”.



803

804 **Figure 5:** TOC and TN concentrations and removal rates during OMBR-RO and
 805 conventional MBR-RO operation. The two systems were operated under the same conditions
 806 as described in the caption of Figure 1.

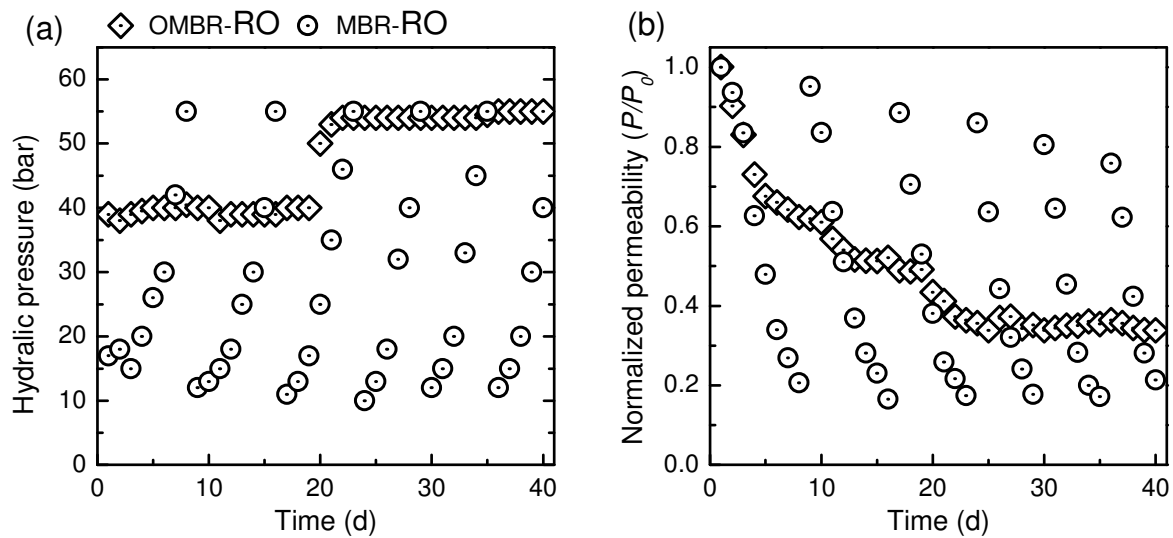
807



808

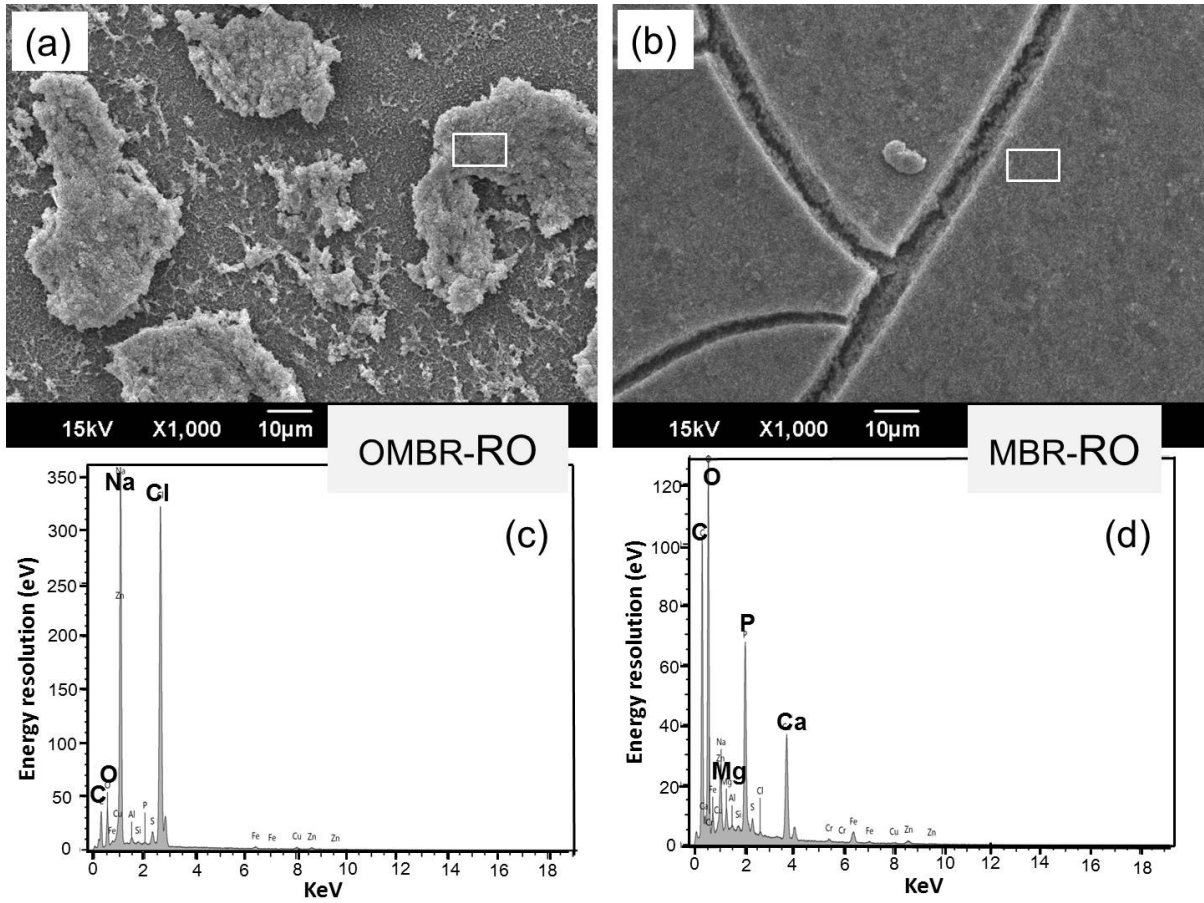
809 **Figure 6:** NH_4^+ and PO_4^{3-} concentrations and removal rates during OMBR-RO and
 810 conventional MBR-RO operation. Experimental conditions are as described in the caption of
 811 Figure 1.

815 their effective octanol-water partition coefficient (Log D) at solution pH 8, the 30 TrOCs investigated were classified as hydrophobic (i.e. Log D
816 > 3.2) and hydrophilic (i.e. Log D < 3.2). Observed TrOC rejection rates do not reflect the real separation capacity of the membranes, but can be
817 used to infer their contributions to TrOC removal in the two hybrid systems. Experimental conditions are as described in the caption of Figure 1.



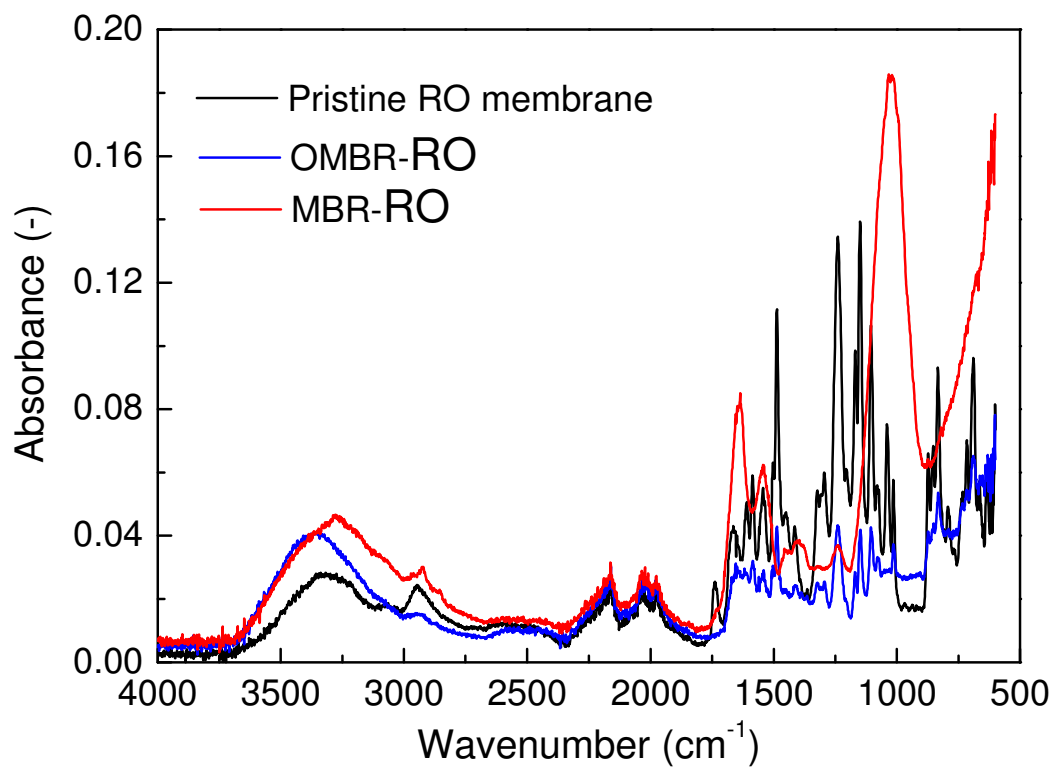
818

819 **Figure 8:** Hydraulic pressure (a) applied to the RO membrane and its normalized
 820 permeability (b) during OMBR-RO and conventional MBR-RO operation. The normalized
 821 water permeability was the ratio of the effective membrane water permeability to the initial
 822 value (P/P_0). Water flux of the RO membranes was adjusted daily to match that of OMBR.
 823 On day 20, 100 g NaCl was added to OMBR draw solution (with constant working volume of
 824 10 L) to replenish draw solute loss. A new RO membrane was used once the membrane
 825 normalized permeability decreased to 0.2. Experimental conditions are as described in the
 826 caption of Figure 1.



827

828 **Figure 9:** (a, b) SEM and (c, d) EDS analyses of the RO membrane surfaces at the
 829 conclusion of OMBR-RO and conventional MBR-RO operation. Experimental conditions
 830 were as described in the caption of Figure 1.



831

832 **Figure 10:** ATR-FTIR absorption spectra of the RO membrane surfaces before and after
833 OMBR-RO and conventional MBR-RO operation. Experimental conditions are as described
834 in the caption of Figure 1.

835